

OPTICAL DESIGN

Spartan IR Camera for the SOAR Telescope

Michael Davis and Edwin Loh
Michigan State University
Loh@pa.msu.edu

10 May, 2001

This document describes the design goals, the optical design, image quality, and optical tolerances of the Spartan Infrared Camera.

1 Design Goals

The high spatial resolution of the telescope is a treasure. With tip-tilt correction, the point-spread function (PSF) is the sum of a diffractive spike and a broader function (Figure 1). A significant amount of light is in the diffraction spike in the H and K bands (Table 1), where the diffraction widths are 0.08 and 0.11 arcsec. The image widths will be between 0.1 and 0.25 arcsec (Figure 2). (Loh 1999.)

The science goals of the Spartan Camera are driven by the high spatial resolution of the telescope. The goals are

- To image in the 1–2.4 μ spectral band over the wide, isokinetic field (5 arcmin diameter) of the tip-tilt corrector.
- To resolve high-contrast features at the diffraction limit, which, for example, is 0.08 arcsec (FWHM) at 1.65 μ .

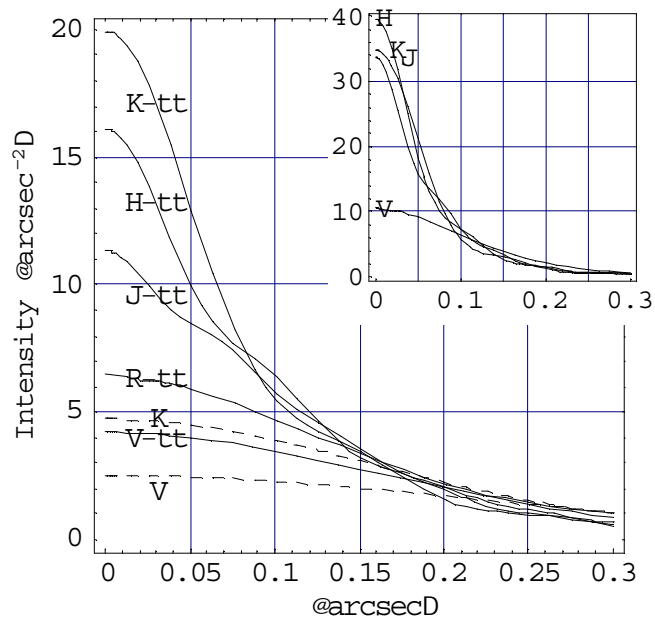


Figure 1 Point-spread functions of the atmosphere with tip/tilt correction (solid lines) and without correction (dashed line) for median seeing. Top quartile seeing is in the inset.

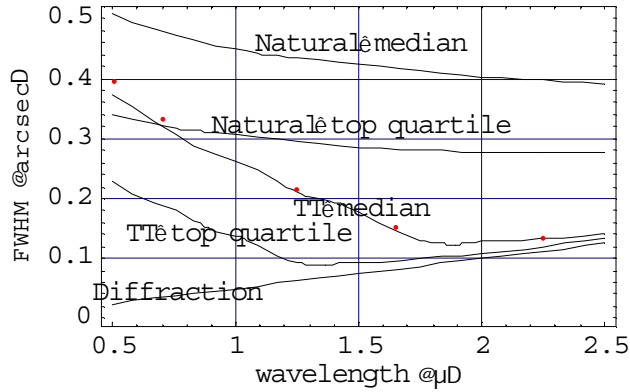


Figure 2 Image width for median and top-quartile seeing with and without tip-tilt correction. Also shown is the diffraction width. For median seeing with tip-tilt correction, the points show the effect of telescope degradation with the Raytheon structure function presented at CDR.

Table 1. Strehl with tip/tilt correction for atmosphere only and for atmosphere and telescope. The loss in Strehl due to the telescope is also shown.

l (m)	Strehl; loss in Strehl		
	Top 25%	Median	
	Atmos.	Atmos.	Atmos + Tele.
0.5	0.0090	0.0036	0.0030; 17%
0.7	0.023	0.0090	0.0078; 14%
1.25	0.15	0.050	0.045; 9%
1.65	0.30	0.12	0.11; 7%
2.25	0.50	0.28	0.27; 5%

2 Optical Design

To meet the design goal of wide field and diffraction-limited resolution, we have developed a novel optical design that uses off-axis collimator and camera mirrors. (See Figure 1.) The camera will have a full set of broadband filters, gratings for limited spectroscopy, and a coronagraph.

The camera has two configurations:

- A high-resolution f/21 mode with 0.04" sampling, which yields a 1.4'×1.4' field of view with a single detector and a 2.8'×2.8' field with four detectors. Pixel sampling is sufficient to resolve the diffraction spike in the H and K bands.
- A wide-field f/11 mode with 0.08" sampling, which yields a 2.7'×2.7' field of view with a single detector and a 5.4'×5.4' field with four detectors. The solid angle coverage is 3 times greater for this mode.

Each configuration utilizes four operating modes:

- Imaging with a choice of 20 filters
- Spectroscopy with a grism without using a slit
- Spectroscopy with a grism using a slit
- Coronagraphy in either imaging or spectroscopic mode for observations of the environs of bright objects.

In the optical design (Figure 3), a collimating mirror and a camera mirror convert the $f/16$ Nasmyth focus to $f/11$ or to $f/21$. To separate the incoming and outgoing beams of these mirrors, these

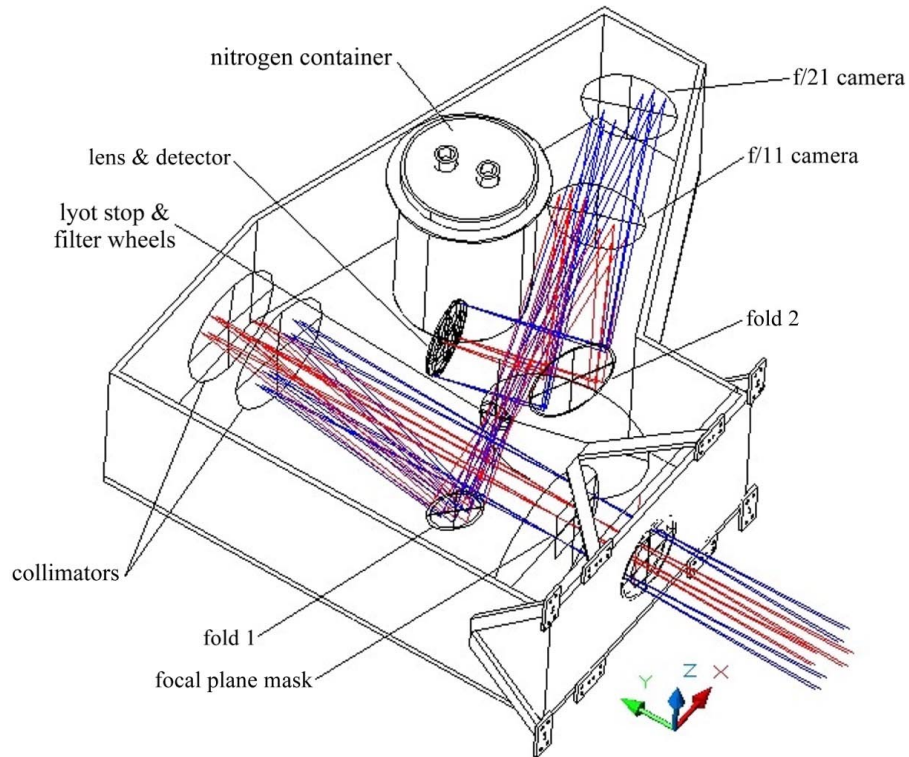


Figure 3 Optical box. Light rays for two field points with the $f/11$ focus are shown in red, and light rays for the $f/21$ focus are in blue. Light enters from the bottom right and traverses the Nasmyth focus and focal plane masks. The light is collimated, reflects off of fold #1, traverses filters, the pupil and Lyot stop, is imaged by either an $f/11$ or an $f/21$ camera mirror, is reflected by fold mirror #2, traverses a field-flattening lens, and comes to a focus. For clarity, the top plate of the optical box is removed. The gravity vector is in the x-y plane. The optical box is attached via four A-frames to the plate that mounts to the telescope. The A-frames are compliant for thermal contraction of the optical box. The tip of each A-frame has a G-10 stub for thermal insulation. The container for liquid nitrogen attaches to both top and bottom plates.

mirrors are off-axis sections of larger parents. The exit pupil is between the collimator and camera mirrors. There is a field-flattening lens very close to the detector plane.

The *infrared detector* is a Rockwell 2048×2048 HgCdTe array. Initially two detectors will be installed. There is space for 4 detectors without modifying the optics.

The *Lyot stops*, one for $f/11$ and one for $f/21$, block light from points outside of the entrance pupil. The pupil is the image of the primary mirror.

Filters and grisms are placed near the pupil. In addition to broadband J, H, and K filters, some narrow band filters will be provided. Grisms allow a spectral resolution $R=380$ at 2 pixels resolution. One grism is needed for each atmospheric window, J, H, and K.

A *field-flattening lens* is near the detector.

To switch between the two plate scales, mechanisms insert or remove the $f/21$ collimator, insert or remove the $f/11$ camera mirror, and rotate the lens-detector assembly by 6° . In addition, Lyot stops change.

The instrument operates at 77 K and the optics are installed at room temperature.

3 Image Quality

The images are diffraction limited. The spot diagrams in Figure 4 are for nine field points at $(n,m)w$, where w is the width of the full field and n and m take on the values $-1/2$, 0, and $+1/2$. The spots are arranged as they appear in the sky.

The Strehl ratio of the instrument, shown in Table 2 for the same field points, are very close to unity. Because the Nyquist criterion, 2 pixels for λ/D , is satisfied only for the $f/21$ channel in the H and K bands, the Strehl ratios need be good only for these cases. For these two cases, the Strehl is at least 0.97, and the instrumental degradation can be made up by an increase of observing time of at most 6%.

Table 2 Strehl ratios for the 9 field points. The sampling of the pixels satisfies the Nyquist criterion only for the underlined cases.

	f/21			f/11		
J	0.980	0.987	0.980	0.892	0.862	0.892
	0.969	0.998	0.969	0.903	0.904	0.903
	0.980	0.945	0.980	0.919	0.977	0.919
H	<u>0.991</u>	<u>0.994</u>	<u>0.991</u>	0.940	0.925	0.940
	<u>0.984</u>	<u>0.999</u>	<u>0.984</u>	0.951	0.941	0.951
	<u>0.991</u>	<u>0.971</u>	<u>0.991</u>	0.957	0.993	0.957
K	<u>0.994</u>	<u>0.996</u>	<u>0.994</u>	0.964	0.956	0.964
	<u>0.990</u>	<u>0.999</u>	<u>0.990</u>	0.971	0.965	0.971
	<u>0.994</u>	<u>0.983</u>	<u>0.994</u>	0.974	0.994	0.974

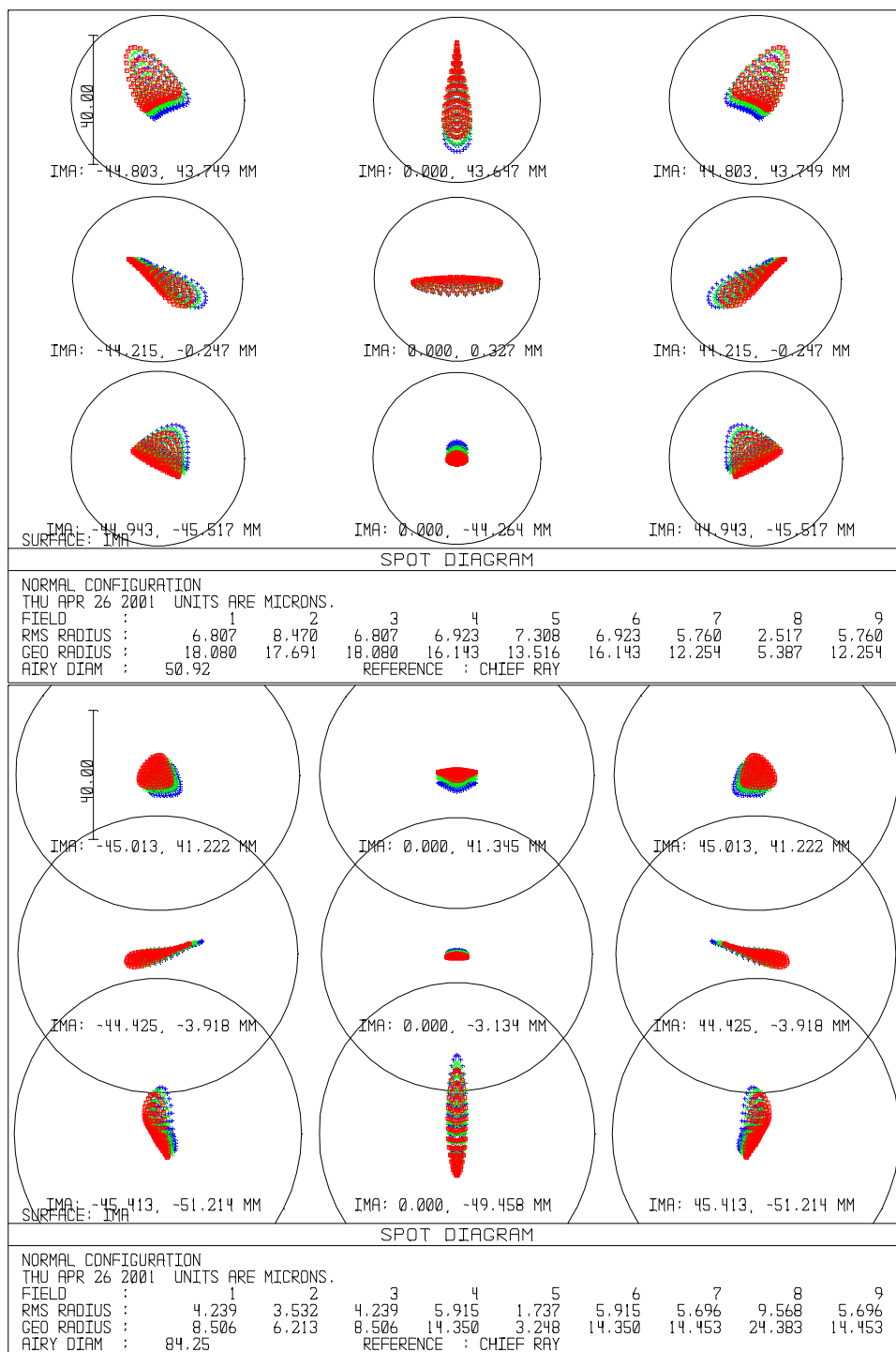


Figure 4 Spot diagram for the f/11 channel (top) and the f/21 channel (bottom) in the H band. Three wavelengths are shown—blue for 1.45μ , green for 1.65μ , and red for 1.85μ . The field points are at (n,m) of the full field for four detectors, where n and m can take the values 0, $-1/2$, and $+1/2$. The circles are the first zero of the Airy function.

4 Tolerances

Three separate tolerances are needed to meet three goals. (1) For sharp images the optics must meet alignment and manufacturing tolerances. (2) To maintain alignment with the tip-tilt guider during operation, the optics must hold position within the boresight tolerances. (3) To minimize the need for relocating the tip-tilt boresight after a change in configuration, the mechanisms should meet a goal for reproducibility. Boresight tolerances are generally tighter than alignment tolerance.

4.1 Alignment Tolerance

The error budget (Table 3) shows the loss in Strehl for alignment, manufacturing errors, and surface irregularity. Surface irregularity is separate because estimating its effect is uncertain.

The instrument has a total of 41 degrees of freedom. The number of positional degrees of freedom is 38. (Each optic has at most 6 degrees of freedom for translation and rotation.) The 3 manufacturing degrees

of freedom are the radius of curvature of the lens and the conic constants of the mirrors. The radii of curvature of the mirrors is not included because errors can be compensated by placement.

The Strehl ratio is allowed to fall by 4% in the H-band due to misalignment and manufacturing errors. By Maréchal's formula (Born & Wolf 1970), the RMS error is $(\ln(1/0.96))^{1/2}/(2\pi)=0.032$ waves. The errors for the degrees of freedom are assumed to add in quadrature. Therefore each degree of freedom is allowed $0.032/(41)^{1/2}=0.0051$ waves.

These tolerances are defined differently: (1) The focal surface is positioned in the directions perpendicular to the optic axis to better than 2% of its size. (2) The z-position and angular tolerance of the telescope focal surface follow the requirement that the loss is less than 1% for an 0.08-arcsec slit.

Table 3 Error budget for the H band.

Quantity	Δ Strehl [mag]
Alignment: 38 parameters	0.042
Manufacturing: 3 parameters	0.003
Surface irregularities	0.016–0.038
Total	0.061–0.083

Some alignment tolerances (Table 4) are tighter than what can be achieved by machining, and optical alignment is required. Most of the positional tolerances are within machining tolerances. The only exception is the position of the detector. Some of the angular tolerances are tight. For example, to achieve 0.17mrad, the rotational tolerance in the x-direction of the first fold mirror, requires 1mil accuracy over 6 inches.

Table 4 Alignment tolerances. The z-direction is along the optic axis. The x-direction is perpendicular to the plates of the optical box.

Element	Positional Tolerance			Angular Tolerance		
	x mm	y mm	z mm	x mrad	y mrad	z mrad
1 Window	NA	NA	NA	NA	NA	NA
2 Focal surface	1.00	1.00	0.30	6.38	6.38	NA
3 f/21 collimator	0.81	0.28	0.19	0.30	0.52	6.10
4 f/11 collimator	0.41	0.15	1.01	0.21	0.42	3.14
5 Fold mirror 1	NA	NA	0.69	0.17	0.26	NA
6 Filter	NA	NA	NA	NA	NA	NA
7 Lyot stop	NA	NA	NA	NA	NA	NA
8 f/21 camera mirror	0.67	0.25	0.40	0.26	0.52	4.80
9 f/11 camera mirror	0.27	0.17	0.49	0.17	0.23	1.86
10 Fold mirror 2	NA	NA	0.16	0.31	0.47	NA
11 Lens	0.48	0.32	0.33	2.27	11.34	NA
12 Detector plane	NA	NA	0.03	0.64	0.64	NA

4.2 Manufacturing Tolerances

Except for the surface irregularity, the manufacturing tolerances were computed in the same way as alignment tolerances. Each degree of freedom is allowed 0.0051 waves.

The tolerances of the radii of curvature of the camera and collimator mirrors are tighter than 0.5%, which is SORL's capability (Space Optics Research Laboratory, 1998). Errors in the radius of curvature can be compensated by the placement of the mirrors. For example, if the radius of curvature of the f/11 collimator is short by 8mm and the collimator mirror is moved by 4mm, the Strehl ratio is the same as that with no radius of curvature error.

Table 5 Manufacturing tolerances.

Element	Radius of Curvature mm	Conic Constant
Primary		
1 Window	∞	
2 f/11 collimator	-1600 ± 2	-1.699 ± 0.002
3 f/21 collimator	-1456 ± 2	-0.720 ± 0.006
4 Fold mirror 1	∞	
5 Filters	∞	
6 f/11 camera	-1249 ± 2	-0.680 ± 0.015
7 f/21 camera	-1983 ± 4	-1.609 ± 0.015
8 Fold mirror 2	∞	
9 Lens, surface 1	220 ± 2	
9 Lens, surface 2	∞	

SORL (2001) is able to meet the tolerances on the conic constants.

4.3 Surface Irregularity

Surface irregularities degrade the Strehl ratio. We estimate this in two ways.

4.3.1 Maréchal's approximation

Maréchal's approximation provides a rough estimate of the ratio Strehl. If the irregularity at two points on the exit pupil are independent, the Strehl decreases by the factor $e^{-\text{var } \phi}$, where $\text{var } \phi$ is the variance of the phase error. Suppose a mirror has a peak-to-valley error of $\lambda/16$, where $\lambda=633\text{nm}$, the wavelength of the HeNe laser. This is the tightest specification for Lambda/Ten (2000). Furthermore suppose peak-to-valley is 4 times the RMS error. Then the RMS surface error is $0.63\mu/16/4$. For a mirror, the phase error doubles because a mirror doubles the path error. For

Table 6 Surface irregularity and loss of Strehl. The surface quality is specified as the peak-to-valley error as a fraction of the wavelength 0.633μ . Two structure functions are used. The surface error is assumed to be independent of separation for the case "flat SF." The functional form of the structure function of the telescope is assumed for the case "real SF."

Element	Quality	Δ Strehl [mag]	
		Flat SF	Real SF
Window	$\lambda/4$	0.0045	0.0004
Collimator	$\lambda/16$	0.0062	0.0032
Fold #1	$\lambda/16$	0.0062	0.0039
Filter	$\lambda/4$	0.0045	0.0037
Camera	$\lambda/16$	0.0062	0.0032
Fold #2	$\lambda/16$	0.0062	0.0013
Lens	$\lambda/4$	0.0045	0.0000
Total		0.038	0.016

a glass element with index $n=1.45$, the phase error is $2\pi(\text{surface error})(1-1/n)/\lambda$ for a single surface.

Achievable manufacturing tolerances and the loss in Strehl are listed in Table 4. With Maréchal's approximation, the total loss in Strehl is 0.038 mag. The contribution for each element is comparable.

For these tolerances, and with the important assumption that the phase errors are independent of separation, the loss in Strehl is 0.038 mag (Table 6).

4.3.2 Structure function

To compute the tolerance on the surface irregularity beyond Maréchal's approximation requires the surface structure function $S(x)$, which is the covariance of the surface error between two points separated by x .

Manufacturers normally specify the peak-to-valley surface error rather than the structure function. We shall use the shape of Raytheon's structure function of the telescope (Raytheon 2000) to estimate the Strehl. To fix the amplitude, we scale this structure function to the specification " λ/N at 0.633μ " namely with $4\text{RMS}=0.633\mu / N$.

The point-spread function of the atmosphere was computed from the modulation-transfer functions of Fried (1966). The modulation transfer function of a perfect telescope is

$$\tau_{\text{diff}}(f) = 2/\pi [\cos^{-1}f - f (1 - f^2)^{1/2}].$$

where f (in cycles) is the spatial frequency normalized to $1/D$. $1 \geq f \geq 0$. The modulation transfer function of the natural atmosphere is

$$\tau_{\text{nat}}(f) = \tau_{\text{diff}}(f) \exp[-3.44 (f D / r_0)^{5/3}].$$

The tip/tilt corrected modulation transfer function is

$$\tau_{\text{tt}}(f) = \tau_{\text{diff}}(f) \exp[-3.44 (f D / r_0)^{5/3} (1 - f^{1/3})].$$

If the optics is not perfect, the modulation transfer function is degraded from $\tau_0(f)$ to

$$\tau(f) = \tau_0(f) \exp[- 1/2 (2\pi/\lambda)^2 S(f D)],$$

where $S(x)$ is the structure function, the mean-square error at separation x . The point spread function is

$$\text{PSF}(\theta) = 2\pi(\lambda/D)^2 \int_0^1 J_0(2\pi\theta D x / \lambda) \tau(x) x dx.$$

Strehl ratio is

$$S = 4\pi^{-1}(D/\lambda)^2 \text{PSF}(0) = 8 \int_0^1 \tau(x) x dx.$$

The loss of Strehl depends of the size of the beam of a single field point compared with the size of the optical element. A small beam samples small separations of the structure function, where the power is lower. Figure 5 shows a representative case for the H band with median seeing.

Four elements—the first fold mirror, the filter, and the collimator and camera

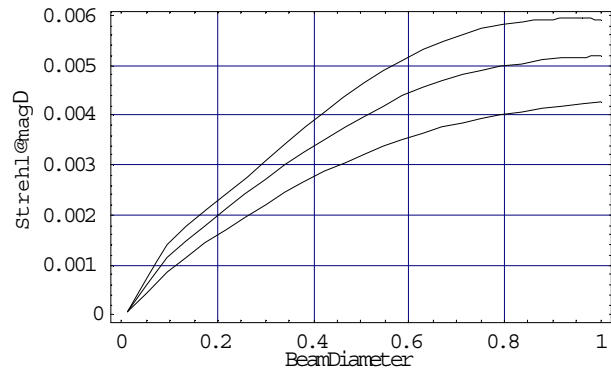


Figure 5 The loss of Strehl vs beam diameter at 1.65m for a mirror with the shape of the Raytheon structure function. The three curves are from top to bottom for no atmosphere, top-quartile seeing, and median seeing. A beam diameter of 1 means the beam fills the optic.

mirrors—dominate the loss of Strehl. (See the 3rd column in Table 6.) For the three mirrors, the beam diameter is 40–50% of the element diameter. The filter, being at the pupil, is fully illuminated. The beam diameter is a small fraction of the element diameter for the others.

The total loss of Strehl is 0.016 mag with this structure function, whereas the estimate from Maréchal’s approximation gives 0.038 mag.

4.4 Alignment Plan

The optics will be aligned with a telescope simulator and a CCD at room temperature. The telescope simulator is described in “SOBER, the SOAR Beam Simulator,” and “Alignment of the Spartan IR Camera” describes a procedure for measuring the relative intensity at 9 field points to determine what needs to move.

Because the aluminum optical box shrinks more than the glass mirrors, the focus will change when the instrument is cooled after alignment. To compensate for this, the f/11 collimator and the f/21 camera mirror will be moved.

4.5 Boresight Tolerance

Boresight alignment means the instrument is aligned with the tip-tilt guider.

4.5.1 Instrument rotation

Boresight must be maintained as the instrument turns.

For the instrument, the goal for the boresight tolerance is to maintain alignment to half the diffraction width in the H-band. This is 0.04arcsec in the sky, which translates to about 1 arcsec for mirrors inside the instrument. We do not have boresight tolerances for the instrument mounting box, which the instrument attaches to, and the tip-tilt sensor. We expect that boresight alignment of all parts to a fraction of the diffraction width will be difficult, and we expect the telescope control system will offset the instrument and tip-tilt sensor with a lookup table to maintain precise boresight alignment.

4.6 Reproducibility with Configuration Changes

Separate requirements apply for changes in the instrument. Suppose the observation is to observe a slit spectrum of a star. The star is positioned by taking pictures. Then the slit is moved into place.

The requirement is that the rotation mechanism for the slit reproduce positions to $\frac{1}{4}$ of the diffraction width in the H band or 7μ .

Change of focal ratio is expected to occur infrequently, and maintaining boresight alignment after a change in focal ratio is desirable but not required. The goal (not requirement) is to reproduce the angular positions of the movable mirrors to maintain positions to $\frac{1}{4}$ of the diffraction width in the H band or 1arcsec for the f/21 collimator and 1.2 arcsec for the f/11 camera mirror.

5 References

Born, M., & Wolf, E. 1970, *Principles of Optics*, Pergamon, New York, p. 468.

Fried, D. L., 1966, JOSA 56, 1372.

Lambda/Ten 2000, <http://www.mcphersoninc.com/lambdaten/lambdaten.htm>

Loh, E, 1999, Image Quality of the SOAR Telescope, unpublished technical report.

Raytheon 2000, SOAR/AOS Critical Design Review.

SORL 1998, private communication.

SORL 2001, private communication.